2016

Fabrication of a tissue- engineered perfusable skin flap

BOSTON UNIVERSITY

SCHOOL OF MEDICINE

Thesis

FABRICATION OF A TISSUE-ENGINEERED PERFUSABLE SKIN FLAP

by

ROSS H. WEINREB

B.S., The Pennsylvania State University, 2014

Submitted in partial fulfillment of the

requirements for the degree of

Master of Science

2016

Approved by

First Reader _____

Matthew D. Layne, Ph.D.
Associate Professor of Biochemistry

Second Reader _____

Jason A. Spector, M.D., F.A.C.S.
Professor of Plastic Surgery and Otolaryngology
Weill Cornell Medical College

ACKNOWLEDGMENTS

FABRICATION OF A TISSUE- ENGINEERED PERFUSABLE SKIN FLAP

ROSS H. WEINREB

ABSTRACT

To date, the reconstructive approach addressing chronic non-healing wounds, deep tissue damage, and severe wound defects relies upon avascular dermal grafts and autologous flap techniques. Such flaps are limited by donor site availability and morbidity, while current dermal grafts rely upon host cellular invasion for neovascularization and incorporation. These products fail to include an inherent vascular network and the supporting cells necessary to ensure adequate incorporation and graft survival beyond the most optimal wound beds. Herein, we fabricate a pre-vascularized full-thickness cellularized skin equivalent containing a three-dimensional vascularized network of interconnected macro and microchannels lined with vascular cells, within a collagen neodermis populated with fibroblasts, and an epidermis comprised of human keratinocytes capable of providing whole tissue perfusion.

Previously, our lab has employed a sacrificial microfiber technique to develop tissue-engineered scaffolds with an inherent hierarchical network of microvessels, which recapitulates the organization of an arteriole, venule, and capillary bed. Utilizing a type-I collagen hydrogel matrix, vascular cells were seeded within pre-fabricated channels and allowed to proliferate to generate an endothelialized microvasculature. These collagen scaffolds were subsequently anastomosed into rat models to demonstrate the clinical feasibility of such approach. The present study aims to more closely recapitulate the *in vivo* structure of human skin via the incorporation of vital epidermal

and dermal components of native skin into a biocompatible construct containing a complex hierarchical vasculature, which may be anastomosed using standard microsurgical techniques and immediately perfused.

Pluronic F127 was used as the sacrificial material: 1.5 mm diameter "U" shaped macrofibers and 100-500 µm-interwoven microfibers were heat extruded and then embedded within type-I collagen into which Cyan Fluorescent Protein (CFP)-tagged human placental pericytes and human foreskin fibroblasts (HFF1) had been encapsulated. Following pluronic sacrifice, resultant channels were intraluminally seeded with Red Fluorescent Protein (RFP)-tagged human aortic smooth muscle cells, Green Fluorescent Protein (GFP)-tagged human umbilical vein endothelial cells, and topically seeded with human epidermal keratinocytes (HEK). Construct microstructure was analyzed using multiphoton microscopy (MPM) after 7, 14 and 28 days of culture. Additionally, after 14 and 28 days of culture, endothelial cells were extracted from the construct using collagenase digestion and Real Time (RT)-qPCR performed to analyze expression of markers of angiogenesis and maturation of the vascular network.

MPM demonstrated a hierarchical vascular network containing macro and microvessels lined by endothelial and smooth muscle cells, supported by perivascular pericytes, all in appropriate microanatomic arrangement. Neodermal HFF1 proliferated throughout the observation period and the HEK neoepidermis developed into a stratified epidermis along the superior aspect of the construct. Angiogenic sprouting from the nascent vascular network into neovessel like structures was noted. RT- qPCR revealed relative expression of Jagged1, Dll4, Ve-Cadherin, and CD31. We have successfully

fabricated a novel tissue-engineered pre-vascularized full thickness skin flap, which recapitulates the inherent hierarchical vasculature found within human skin and is suitable for *in vivo* perfusion. We provide the platform for an on- demand, geometrically tunable tissue engineered skin equivalent with an anastomosable vascular network. This tissue-engineered skin flap holds the potential to transform reconstructive surgical practice by eliminating the consequences of donor site morbidity, and enabling rationally designed, patient-specific flaps for each unique wound environment and anatomic location.

TABLE OF CONTENTS

LIST OF TABLES

LIST OF FIGURES

LIST OF ABBREVIATIONS

ECM .... Extracellular Matrix

FBS .... Fetal Bovine Serum

HASMC-RFP .... Human Aortic Smooth Muscle Cells- Red Fluorescent Protein

HEK .... Human Epidermal Keratinocytes

HFF1 .... Human Foreskin Fibroblasts

HPLP-CFP .... Human Placental Pericytes- Cyan-Fluorescent Protein

HUVEC-GFP .... Human Umbilical Vein Endothelial Cells- Green Fluorescent Protein

MACS .... Magnetic- Activated Cell Sorting

MPM .... Multi-Photon Microscopy

P/S .... Penicillin/ Streptomycin

PDMS .... Polydimethylsiloxane

PMTs .... Photomultiplier Tubes

vSMC .... Vascular Smooth Muscle Cells

INTRODUCTION

Overall, tissue loss resulting from traumatic injury or surgical resection is one of the foremost problems facing health care today, accounting for about one half of the total annual expenditures in health care in the US (Devices, 2000). More specifically, open deep tissue wounds resulting from chronic non-healing wounds, severe soft tissue infections and large defects following oncologic resection or traumatic injury is estimated to affect nearly 65 million Americans at an annual cost of $25 billion dollars (Sen et al., 2009). The impact of wounds is seen both economically and psychologically, as patients living with both acute and chronic wounds experience anxiety, depression, pain and embarrassment (Patterson et al., 1993; "The economic cost of wound care | Smith & Nephew," n.d.).

While treatment requires a multidisciplinary approach, it is frequently the role of the plastic and reconstructive surgeon to address these types of complex wounds and injuries. Derived from the Greek word "*plastikos,*" plastic surgery represents the field of medicine which deals with correcting and reconstructing body parts secondary to injury, birth or cosmetic defects with the overarching goal of restoring form and function (Pećanac, 2015). Plastic surgeons rely upon the "reconstructive ladder" (Figure 1) to address the management of these increasingly complex wounds, which is a systematic approach that allows the plastic surgeon to proceed through a cognitive, step-wise progression of reconstructive options to select the most suitable reconstructive technique to various wounds— the more complex and problematic the wound, the higher up the ladder the surgeon usually must climb (Boyce & Shokrollahi, 2006).
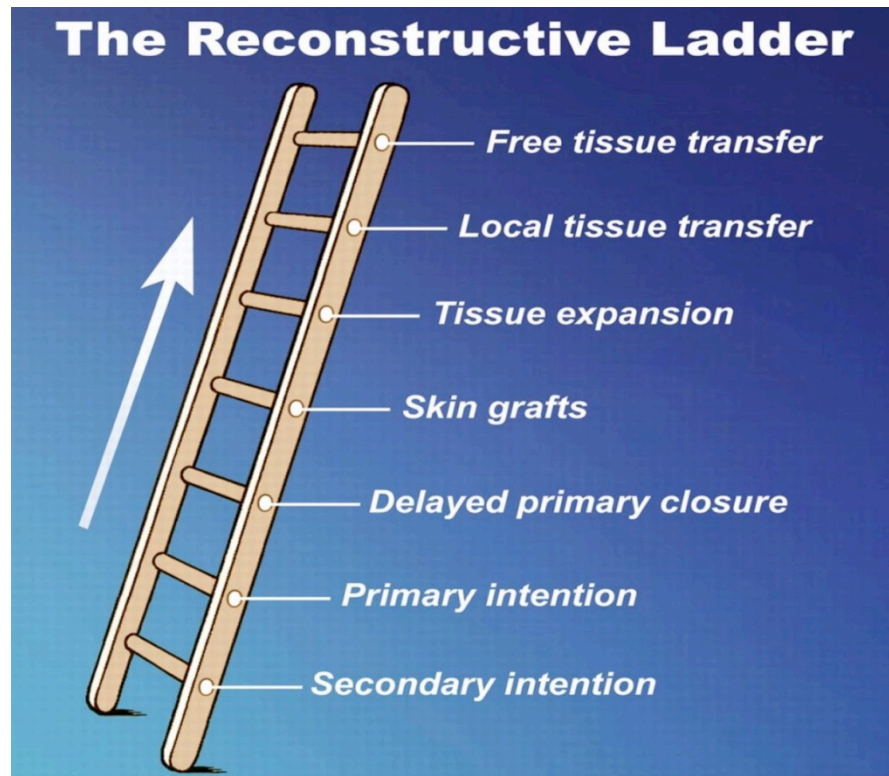
1

Figure 1. The Reconstructive Ladder: Step-wise reconstructive approach utilized by plastic and reconstructive surgeons to address various types of soft tissue defects encountered in clinical practice. Original image from: Boyce & Shokrollahi, 2006. Reconstructive Surgery.

Wounds may be left alone to close by themselves, which describes secondary intention or they will be closed by primary intention, which includes basic suturing. However, when wounds fail to heal by primary or secondary intention, the surgeon will consider the use of a skin graft or flap. Typically used for wounds with optimal wound beds, a skin graft is harvested from a donor site and then transferred to the recipient site without carrying its inherent blood supply. Therefore, a graft, which is avascular, relies upon host cellular invasion for neovascularization and incorporation ("Chapter 2 grafts and flaps," n.d.). Skin flaps, which are used in sub optimal wound beds, are slabs of tissue

that maintain their own blood supply by either remaining attached to the donor site vasculature (pedicled flap) or moved to a new site where the blood vessel is surgically reconnected. The latter details a more complex approach known as an autologous free tissue transfer, which is used for intricate wounds with complex wound beds unable to support a skin graft (Boyce & Shokrollahi, 2006; Kannan et al., 2005).

Expert microvascular surgery enables the transfer of these thick autologous tissue flaps via the vascular dissection and detachment of an isolated and specific region of the body (eg, skin, fat, muscle, bone) and transfer of said tissue to another region of the body, with anastomosis of the divided artery and vein to a separate recipient artery and vein located at the site of the defect (Adams & Ramsey, 2005; Andreassi et al., 2005; "Free Tissue Transfer Flaps: Definition, Indications, Preoperative Considerations," n.d.) (Figure 2). Clinically vascularized tissue flap transfers incorporate surgically anastomosable (>1 mm) feeder vessels with their downstream branched network intact within the tissue bulk (Lokmic et al., 2007). This configuration ensures whole tissue perfusion upon vascular anastomosis, however serious donor site morbidities, which include ischemia, deep vein thrombosis, sensory nerve loss/damage and or delayed healing can diminish the utility of this procedure (Fimiani et al., 2005) (Figure 3).

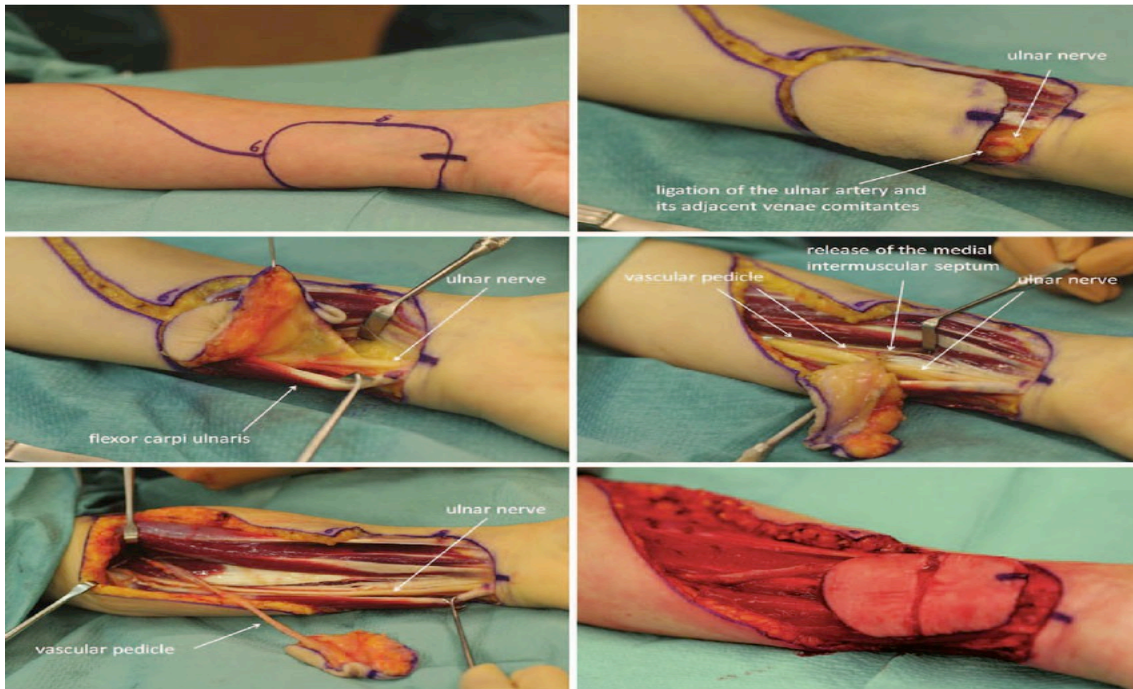**Figure 2. Ulnar Forearm Free Flap:** Design, incision, elevation and dissection of ulnar forearm free flap. Original image from: Hekner et al., 2013. Plastic and Reconstructive Surgery.

Figure 3. Donor Site Morbidity: Following a radial forearm flap healing is unfavorable and considerate aesthetic deformation exists. Original image from: Hekner et al., 2013. Plastic and Reconstructive Surgery.

There is therefore an increased need for biocompatible, tissue-engineered skin substitutes to address complex reconstructive challenges resulting from organ failure, chronic non-healing wounds, severe soft tissue infections and large defects following oncologic resection or traumatic injury.

The field of tissue engineering and regenerative medicine combines the fields of biology, engineering and polymer chemistry to develop functional tissues that restore, maintain, and improve damaged tissues or whole organs. This field is emerging as a potential alternative or even a complementary solution to address the aforementioned failures whereby fully functional natural, synthetic, or semisynthetic tissue equivalents are implanted to restore the native tissues functionality (Devices, 2000). Focused on the development of tissue engineered skin grafts, the current commercially available products are avascular and lack the patent, fully perfusing vascular supply of native tissue, which is critical to the engraftment and survival of replacement bulk tissue (Kojima et al., 2002; Novosel, Kleinhans, & Kluger, 2011).

As leaders in the field of tissue engineered skin, Rheinwald and Green were one of the first to demonstrate the ability to isolate, cultivate, and expand human epidermal keratinocytes from a small skin biopsy to grow skin epidermis. This breakthrough led to the development of the first-cell based tissue engineered product, Epicel™, which consists of sheets of autologous keratinocytes that are used to cover large areas of the skin of patients suffering from catastrophic injuries who do not have enough viable skin remaining to be treated with traditional autografting techniques. However, this product is not only expensive but extremely fragile, only a few cells thick and does not contain a

5

dermis and therefore rarely used (Berthiaume, Maguire, & Yarmush, 2011).

Yannas and Burke later developed a novel product consisting of type-I bovine collagen and shark chondroitin. This mixture, later cross-linked into a porous matrix contains a silicone sheet attached on one side to function as a temporary epidermis-like barrier. The matrix is biocompatible and biodegradable and eventually disappears as the host cells invade and deposit their own extracellular matrix (ECM) creating a neodermis made of the patient's own cells. Subsequently, the silicone sheet is removed and the wound is covered with a skin graft. This product, know as Integra™, is used to cover severe wounds where the damage extends deep into the dermis. Integra™ contains no living cells and no inherent vascular network therefore limiting its use only to optimal wound beds. As a result of product avascularity, Integra™ relies upon host cellular invasion for neovascularization and incorporation, which is a lengthy process and exposes the patient to a number of complications that may lead to infection and graft loss (Berthiaume, Maguire, & Yarmush, 2011) (Figure 4).

Apligraf™, developed by Eugene Bell is a composite skin graft containing both dermal and epidermal elements. Initially, a collagen gel is seeded with dermal fibroblasts to develop into a neodermis after which keratinocytes are seeded topically to form a keratinized neoepidermal layer. This product utilizes allogeneic cells isolated from neonatal human foreskin, which provides the potential for off-the-shelf availability. However, the allogeneic skin substitute can provide only temporary coverage, as the patient will eventually reject it (Berthiaume, Maguire, & Yarmush, 2011).

The commercially available artificial tissue grafts are thin (<2 mm), acellular, and

are poorly if at all revascularized by chronically ill or radiated patients, resulting in limited use beyond skin replacement in the most optimal wound beds (Callcut et al., 2006; Reiffel et al., 2012; Zhong, Zhang, & Lim, 2010). As cells must lie within 200-300 μm of the nearest capillary in order to receive both the oxygen and nutrients necessary for survival tissues also require an intact microvascular network to ensure adequate transfer of nutrients and oxygen for survival (Greene, 1941). Therefore, several approaches have been employed that take advantage of vasculogenesis to bioengineer vascular networks within biocompatible scaffolds by encapsulating vascular cells within to allow for self-assembly into perfusable microvascular networks (Hoying, Utzinger, & Weiss, 2014; Wu et al., 2004). However, this spontaneous vascular self-assembly through endothelial/mural cell polycultures within biocompatible matrices create hemodynamically inefficient capillary beds with uniformly small diameters that at best can inosculate with host capillaries and thus only be applied as would a skin graft (Chen et al., 2012; Gauvin et al., 2010). Furthermore, the functionality of a clinically translatable tissue engineered skin flap relies upon the necessary architecture to be surgically anastomosed to the host vasculature, which these approaches fail to recognize.
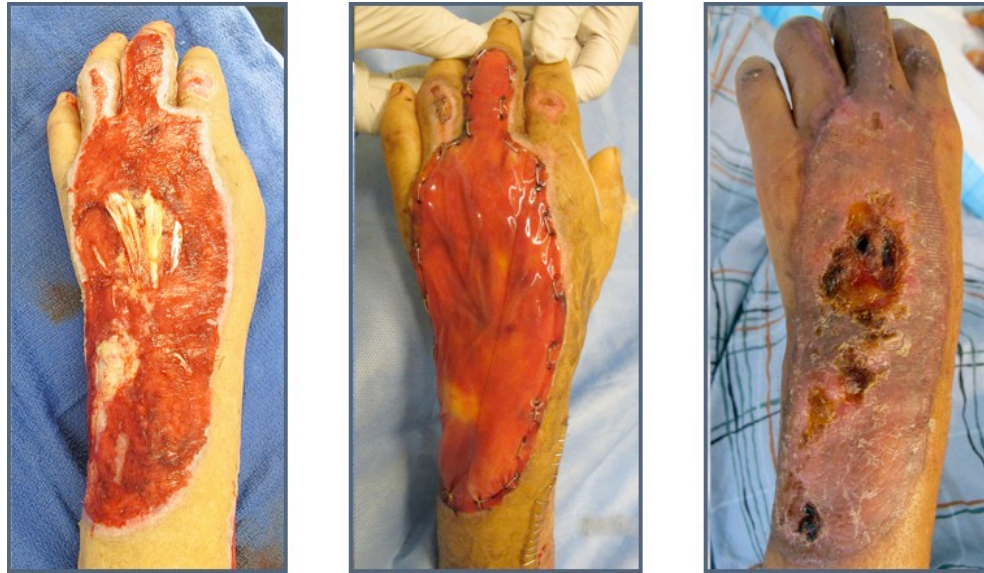
Figure 4. Graft Rejection: Depicted here is the progression of graft failure when Integra was used in a sub-optimal wound bed. Original image obtained from Jason A. Spector, MD, FACS.

Current tissue engineering vascularized tissue fabrication strategies focus on incomplete and extreme scales, and are divided into three regimes: single straight small diameter sized vessels (2-5 mm), self-directed vasculogenesis within hydrogels, and microfabricated vascular networks (Baek et al., 2013; Blinder, Mooney, & Levenberg, 2014; Golden & Tien, 2007; Hasan et al., 2014; Jiang & Luo, 2013; Lee et al., 2014; Lin et al., 2013). The methodologies utilized to achieve these fail to produce 1) macro-scale (0.5-2.0 mm) vascular networks and 2) the primary branch order networks, both of which are essential for perfusing whole large tissue volumes with minimal vascular resistance (Kim et al., 2014). Moreover, approaches that generate vascularized microscale tissue elements (<1 cm^3 and ~1 mm thick) that result in capillary microvasculature of uniform diameter with very high vascular resistance are useful for *in vitro* mechanistic study and drug screening, but they are not clinically translatable because their size is restricted,

require a non-biocompatible support frame, and cannot be surgically anastomosed (Ehsan et al., 2014; Kolesky et al., 2014; Miller et al., 2012; Tremblay et al., 2005). These current strategies fail to recognize the clinically translatability when developing thick tissue replacements (>1 mm) as such engineered constructs would not be able to be immediately perfused by microsurgical anastomosis, and thus would be bound by the same constraints as all grafted tissue.

The availability of an on-demand, geometrically tunable tissue engineered equivalent with an anastomosable inherent vascular network would transform reconstructive surgical practice by eliminating the consequences of donor site morbidity and enabling rationally designed, patient specific flaps for each unique wound environment and anatomic location.

SPECIFIC AIMS

Our lab has previously employed a sacrificial microfiber technique to develop a tissue-engineered scaffold with an inherent hierarchical network of microvessels, which recapitulates the organization of an arteriole, venule, and capillary bed. Utilizing a type-I collagen hydrogel matrix, vascular cells were seeded within pre-fabricated channels and allowed to proliferate to generate pre-vascularized microvessels. These vascularized collagen scaffolds were subsequently anastomosed into rat models to demonstrate the potential clinical translation of such an approach (Hooper et al., 2014). Herein, we endeavor to fabricate a clinically translatable tissue-engineered skin flap comprised of a collagen neodermis containing a pre-fabricated hierarchical network of vascularized vessels and vital epidermal and dermal components of the native skin.

Towards this end we will:

1. Fabricate a pre-vascularized three-dimensional skin equivalent containing a hierarchical network of vascularized microvessels seeded with human vascular cells encapsulated within a type-I collagen bulk containing fibroblasts, perivascular pericytes and an epidermis comprised of human keratinocytes.

2. Utilize Multiphoton Microscopy to determine the hierarchal organization of the vascular network within our tissue engineered skin flap.

3. Within our tissue-engineered constructs evaluate endothelial cell expression of genes associated with angiogenesis and vessel maturation.

This approach carefully considers the impact that such a tissue engineered skin flap will have throughout the field of plastic and reconstructive surgery. We hope that this research will impact the field of reconstructive surgery by offering an available *de novo* designable vascularized tissue that obviates the need for autologous tissue harvest.

METHODS

Collagen Extraction:

Tendons were harvested from frozen rat tails (Pel- Freeze® Biologics, Rogers, AK) and suspended in 0.1% acetic acid to create a concentration of 75 mL/g of tendon. After 72 hours at 4°C, the solution was centrifuged for 90 min at 8800xg. The supernatant was collected, frozen and lyophilized. The lyophilized collagen was further suspended in 0.1% acetic acid to create a 15 mg/mL type-I collagen stock solution and stored at 4°C.

Cell Culture:

Angiocrine Bioscience from Weill Cornell Medical College graciously provided Red Fluorescent Protein-tagged human aortic smooth muscle cells (HASMC-RFP) and Green Fluorescent Protein -tagged human umbilical vein endothelial cells (HUVEC-GFP). HUVEC-GFP were cultured using endothelial cell basal media supplemented with endothelial mitogen (Promocell, Heidelberg, Germany), and penicillin/streptomycin (P/S), while HASMC-RFP were cultured in smooth muscle cell basal media supplemented with smooth muscle cell mitogen (Promocell, Heidelberg, Germany) and P/S. Human foreskin fibroblasts (HFF1) (Promocell, Heidelberg, Germany) were cultured in Media 199x supplemented with fetal bovine serum (FBS, Hyclone©, Thermo Scientific, Logan, UT) and P/S. Human placental pericytes (HPLP) (Promocell, Heidelberg, Germany) were cultured using pericyte cell basal media supplemented with pericyte mitogen (Promocell, Heidelberg, Germany), and P/S. HPLP were transfected using a pre-made purified eCyan

Fluorescent Protein (eCFP) lentivirus (eCFP Lentifect™, Genecopoeia, Rockville, MD) prior to use. Human epidermal keratinocytes (Promocell, Heidelberg, Germany), were cultured using keratinocyte cell basal media supplemented with keratinocyte mitogen, $CaCl_2$ (Promocell, Heidelberg, Germany), and P/S. All cell lines were maintained under standard cell culture conditions with media changes every other day.

Sacrificial Macrofiber and Microfiber Fabrication:

A negative 1.5 mm "U" shaped pattern was created within a Polydimethylsiloxane (PDMS) mold (Figure 5a). A sacrificial polymer, Pluronic® F127 (Sigma Aldrich®, St. Louis, MO) was heated to 70°C and poured into the pre-patterned PDMS mold. After solidification at 4°C for 10 minutes, the macrofibers were demolded (Figure 5b). Pluronic® F127 was manual extruded to create the dense three-dimensional interconnected microfiber matrices with channel sizes ranging from 100-500 μm (Figure 5c). The three-dimensional Pluronic® F127 microfiber network was melt fused to the Pluronic® F127 macrofibers to recapitulate the hierarchical organization of an *in vivo* arteriole, capillary bed, and venule (Figure 5d).

Scaffold Preparation:

A PDMS mold was used to create adjacent 15 mm x 15 mm x 5 mm reservoirs, which were connected by inlet and outlet channels. Fourteen-gauge catheters were placed into both channels to suspend the sacrificial network above the reservoir (Figure 5e). The catheters provide an adequate and efficient attachment site for *in vivo* surgical anastomosis. The PDMS mold and Pluronic® F127 network was sterilized under ultra-violet light for 24 hours prior to use. Under sterile conditions, the aforementioned type-I collagen was neutralized on ice using Medium 199 (Gibco®, Life technologies, Grand Island, NY) and NaOH to a final concentration of 0.9 mg/mL and pH 7.4. Concurrently, HFF1 and HPLP-CFP were split using Accutase® (BioLegend, San Diego, CA) and counted using a standard hemocytometer. Cellular encapsulated collagen was prepared with the addition of $1x10^6$ HFF1 and $1x10^6$ HPLP-CFP for every 1 mL of neutralized collagen prior to thermal gelation. The HFF1/HPLP-CFP collagen mixture was manually extruded over the sacrificial microfiber network and allowed to undergo thermal gelation at 37°C for 45 minutes. After which, a 1:1 ratio of fibroblast to pericyte media was added to allow for overnight Pluronic® F127 network sacrifice.
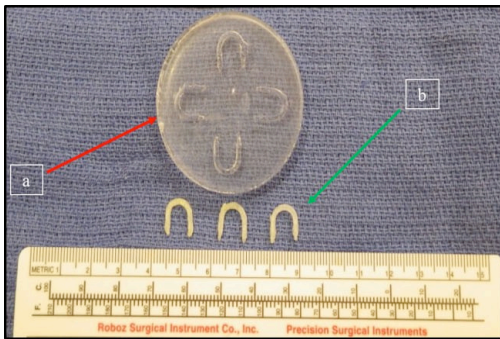
Figure 5a/b. Scaffold and Network Prepartion: Polydimethylsiloxane (PDMS) molds for fabrication of "U" shaped Pluronic® F127 macrochannel (red arrow). **5b)** De- molded "U" shaped Pluronic® F127 macrochannel (green arrow).

Figure 5c: Manually extruded Pluronic® F127 will be sacrificed in type-I collagen to create the microchannels.

Figure 5d): Pluronic® F12 "U" shaped macrochannel melt fused to manually extruded Pluronic® F127 to form the macro and microchannel network.
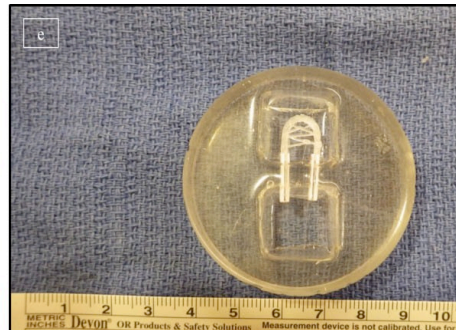

Figure 5e: PDMS molds used to house the collagen hydrogel. 14- gauge catheters are used for inlet and outlet ports.

Scaffold Seeding:

Following overnight sacrifice, the scaffolds were prepared for intraluminal seeding. 150 µl of $5x10^5$ HASMC-RFP were slowly injected into the scaffolds inlet channel, and twenty-four hours thereafter 150 µl of $5x10^5$ HUVEC-GFP were slowly injected into the same channel. Finally, 100 µl of $1x10^6$ cells HEK were topically seeded onto the construct. Forty-eight hours later, collagen skin hydrogels were individually transferred to 30 mL freestanding centrifuge tubes (Evergreen Scientific, Los Angeles, CA) and incubated at 37°C. Samples were cultured in a 1:1 ratio of HUVEC to pericyte media for 7, 14, and 28 days with daily media changes. A total of 20 hydrogels were prepared and seeded.

Multiphoton Microscopy:

An upright Olympus FluoView FV1000MPE multiphoton microscope was used to image each skin construct containing live cells. Prior to imaging, HBSS was injected into the channel network of each hydrogel to keep the channels patent. All specimens remained within their PDMS mold and a drop of phosphate buffered solution was added topically to achieve water immersion of the microscope objective. A tunable mode-locked femtosecond pulsed Ti-Sapphire laser (Mai Tai DeepSee, Spectra-Physics, Newport Corporation, Santa Clara, CA) was used to excite the samples at 810 nm. An area of 1.27 mm x 1.27 mm of the sample was imaged up to a maximum depth of ~1 mm from the surface in 5-20 µm steps. All images were acquired using a 10X/0.6 NA water immersion objective, which is corrected for transmittance of a broad range of wavelengths from UV

to near-IR. Images were collected using three multialkali photomultiplier tubes (PMTs), each of which collected one of the signals of interest. Specifically, the CFP signal was collected at 420-460 nm, GFP at 495-540 nm, and RFP at 575-630 nm. Unseeded constructs with sacrificed networks were filled with 5μm green fluorescent microspheres (Sigma Aldrich, St. Louis, MO).

Multiphoton Image Analysis:

All multiphoton images acquired were analyzed either with Imaris™ (Bitplane USA, Concord, MA) or Metamorph™ (Molecular Devices, Sunnyvale, CA). Specifically, Metamorph™ was used for all image analysis and quantification of channel dimensions, whereas Imaris™ was used for the visualization of the 3D image volume.

Collagenase Digestion and Cell Sorting:

A collagenase solution of Collagenase A, Dispase II, and DNase was prepared in a buffered solution of NaCl (140mM), KCl (5mM), Phosphate Buffer (2.5mM), Hepes (10mM), $CacCl_2$ (2.0mM) and $MgCl_2$ (1.3mM). Using single edged industrial razor blades (VWR, West Chester, PA), 14 day and 28 day skin hydrogels were minced into smaller pieces. The minced hydrogels were added into a mixed solution of 2 mL collagenase and 6 mL Medium 199 (1:3 ratio of collagenase to M199). This mixture was placed in a 37°C rotational incubator for approximately 45-60 minutes. After which, the solution was filtered through a 100 μm EASYstrainer™ (Greiner Bio-One, Monroe, NC) and

subsequently centrifuged at 1000 RPM for 5 min. The remaining cell pellet was re-suspended in 50 µl Magnetic-Activated Cell Sorting (MACS) buffer to prepare the sample for cell sorting, and CD31-FITC antibodies (eBioscience, San Diego, CA) were added to the mixture as recommended by manufacture. The sample was sorted based on CD31+ labeled endothelial cells using a FACSJazz cell sorter (BD Biosciences, San Jose, CA).

RNA Extraction cDNA Synthesis:

Total RNA was extracted from endothelial cells from 14 day, and 28 day skin hydrogels using RNAeasy Microkit® (Qiagen, Hilden Germany) following the manufacturer's instructions. The concentration of total RNA extracted was determined using UV absorption with a NanoDrop1000 spectrophotometer (Thermo Scientific, Waltham, MA). A two-step qRT-PCR assay was performed where cDNA was synthesized from the total RNA sample using qScript™ cDNA SuperMix (Quanta Bioscience, Gaithersburg, MD) as per the manufactures instructions, after which RT-qPCR was performed.

Primers and Quantitative PCR:

Endothelial expression of Jagged1, Dll4, CD31, VE-Cadherin, α-SMA, and 18S rRNA were analyzed from 14 day, and 28 day skin samples, and normalized to the 18S rRNA reference gene. All primers were graciously provided by Dr. Shahin Rafii of Weill Cornell Medical College (Table 1). Quantitative RT-PCR for the relative expression analysis of selected genes was carried out using the KAPA SYBR® fast master mix (Kapa

Biosystems, Wilmington, MA). A master mix was prepared for each target gene comprising 2X SYBR Green master mix, each forward and reverse primer (2.5μM working concentration) and cDNA, up to a total reaction volume of 15 μl. PCR cycling parameters were as follows; denaturation at 95°C for 3min followed by 40 cycles of 95°C for 3s and 60°C for 20s. Product specificity was evaluated by melting curves. Each total RNA sample was amplified in duplicates and the mean values were used for further analysis.

Table 1: Human primers for RT-qPCR

Primer	Sequence
Jagged1	**F:** 5'-TGACCAGAATGGCAACAAAA-3'
	R: 5'-GGGTGTGGGATGCACTTATC-3'
Dll4	**F:** 5'-GCGAGAAGAAAGTGGACAGC-3'
	R: 5'-ATTCTCCAGGTCATGGCAAG-3'
VE- Cadherin	**F:** 5'-TTGGAACCAGATGCACATTGAT-3'
	R: 5'-TCTTGCGACTCACGCTTGAC-3'
CD31	**F:** 5'-ACCGTGACGGAATCCTTCTCT-3'
	R: 5'-GCTGGACTCCACTTTGCAC-3'
α-SMA	**F:** 5'-AAAAGCAAGTCCTCCAGCGTT-3'
	R: 5'-GAGCCATTGTCACACACCAAG-3'
18S rRNA	**F:** 5'-AGTCCCTGCCCTTTGTACACA-3'
	R: 5'-CCGAGGGCCTCACTAAAC-3'

RESULTS

The three-dimensional Pluronic F127® network of interconnected microfibers consistently sacrificed to form a dense array of continuous and patent microchannels within our collagen hydrogels. Both media perfusion prior to intraluminal cell seeding and MPM imaging of seeded and unseeded skin constructs confirmed intact bridging connections between the microchannel network and the inlet and outlet macrochannels (Figure 6).

Multiphoton microscopy was used to identify the three-dimensional hierarchical organization of the interconnected microvessels in both seeded and unseeded constructs. The images reveal microvessels of varying diameters each with a patent and continuous lumen connecting microchannel to adjacent microchannel (Figure 7). Microchannel diameters were manually measured, documented, and exported to Microsoft Excel™. The data set of channel diameters is plotted as a frequency distribution for all samples used within this study (Figure 8). The microchannels range in size from 30 μm to 500 μm, with an average channel size of 184 μm.
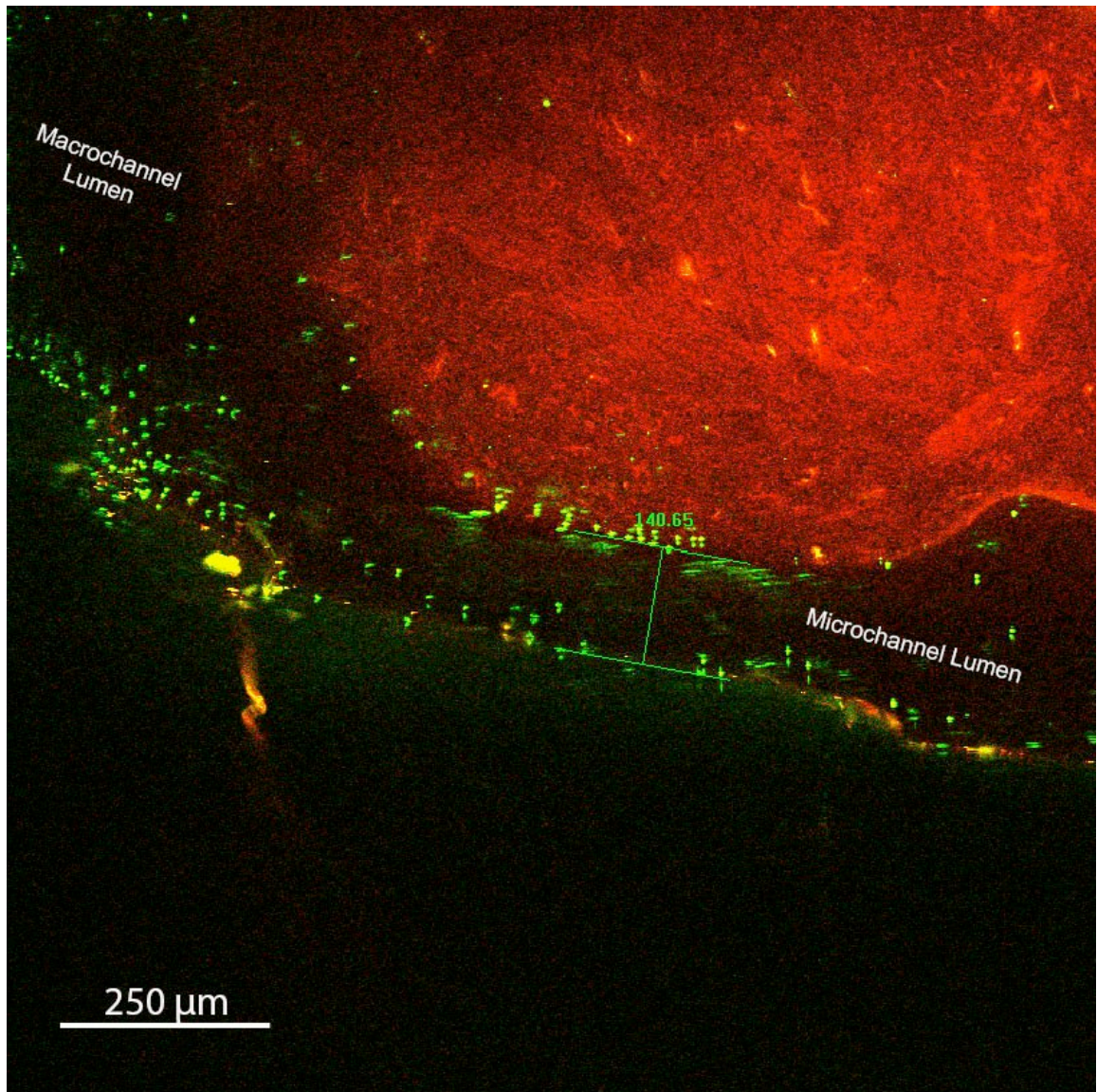
Figure 6. MPM imaging of Unseeded Microchannel: 10x/0.6NA water immersion objective MPM imaging of unseeded sacrificed microchannel, perfused with green fluorospheres, connecting the larger macrochannel Collagen bulk fluorescing red to provides contrast.
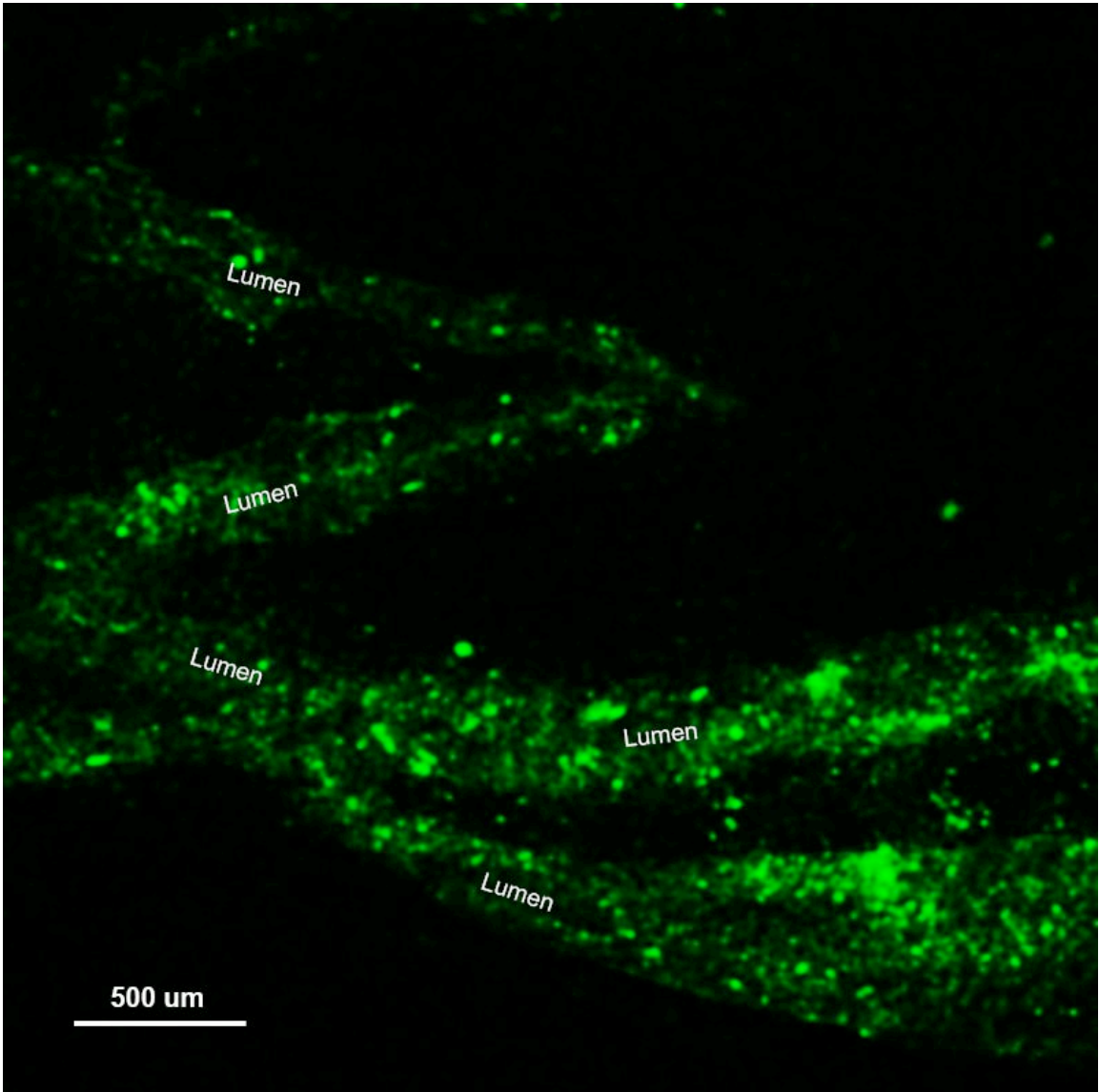
Figure 7. MPM imaging of Unseeded Interconnected Microchannels: 10x/0.6NA water immersion objective MPM imaging of unseeded sacrificed microchannels perfused with green fluorospheres.
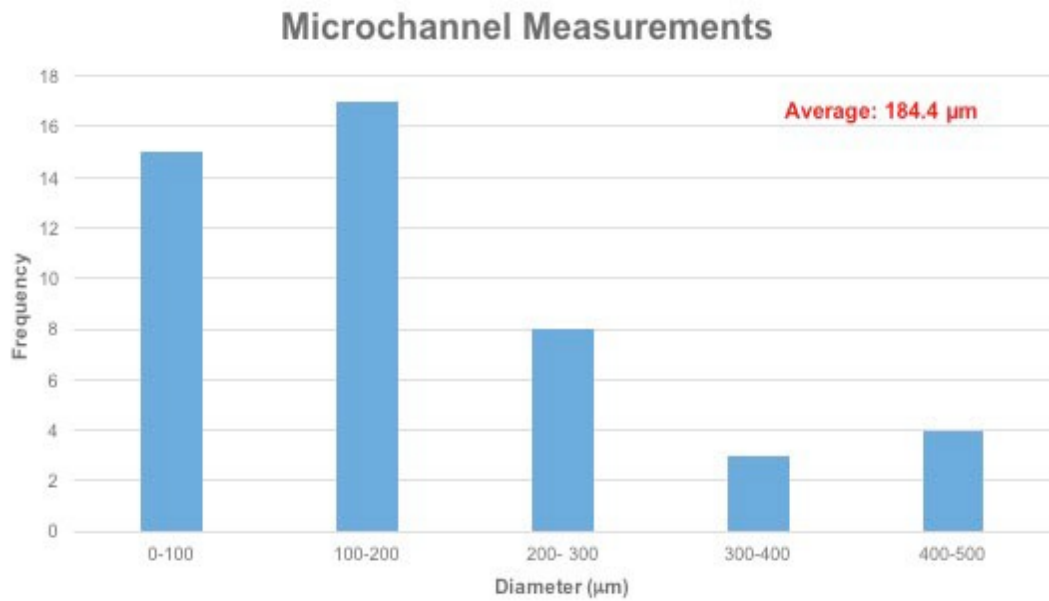
Figure 8. Histogram of Microchannel Measurements:
Frequency distribution for the diameters of Pluronic® F127
microchannels. measured.

We analyzed the coverage of the endothelial-lined microvessels by mural cells, namely vascular smooth muscle cells (vSMCs) and pericytes following 7, 14 and 28 days of culture. MPM imaging confirmed the presence of single layer thick endothelial lining along the microchannel luminal surface with a carpet of smooth muscle cells sub adjacent to the luminal surface. This spontaneous organization of cells into the appropriate anatomical arrangement was more evident at 14 and 28 days (Figure 9). MPM imaging of these samples reveal a three-dimensional network of interconnected microchannels lined with cells anatomically arranged to form an identifiable neointima of HUVEC-GFP and neomedia of HASMC-RFP with perivascular supporting HPLP-CFP (Figure 10a-c).

Pericyte proliferation is seen to increase from day 7 through day 14 evident by the spatial arrangement of perivascular supporting cells surrounding the endothelial-lined microchannel. Following 14 days of culture, sprouting morphogenesis was visualized using MPM imaging (Figure 11). Notably, imaging after 28 days of culture revealed endothelial neovessels from our pre-fabricated microvascular connections. Furthermore, GFP-HUVEC lined neovessels were identified in areas of the hydrogel void of any pre-fabricated microvasculature indicating spontaneous endothelial cell tube formation within our pre-vascularized skin flap (Figure 12). The neovessels were predominantly composed of endothelial cells and supported by smooth muscle cells and perivascular pericytes in anatomically appropriate position (Figure 13a-b).
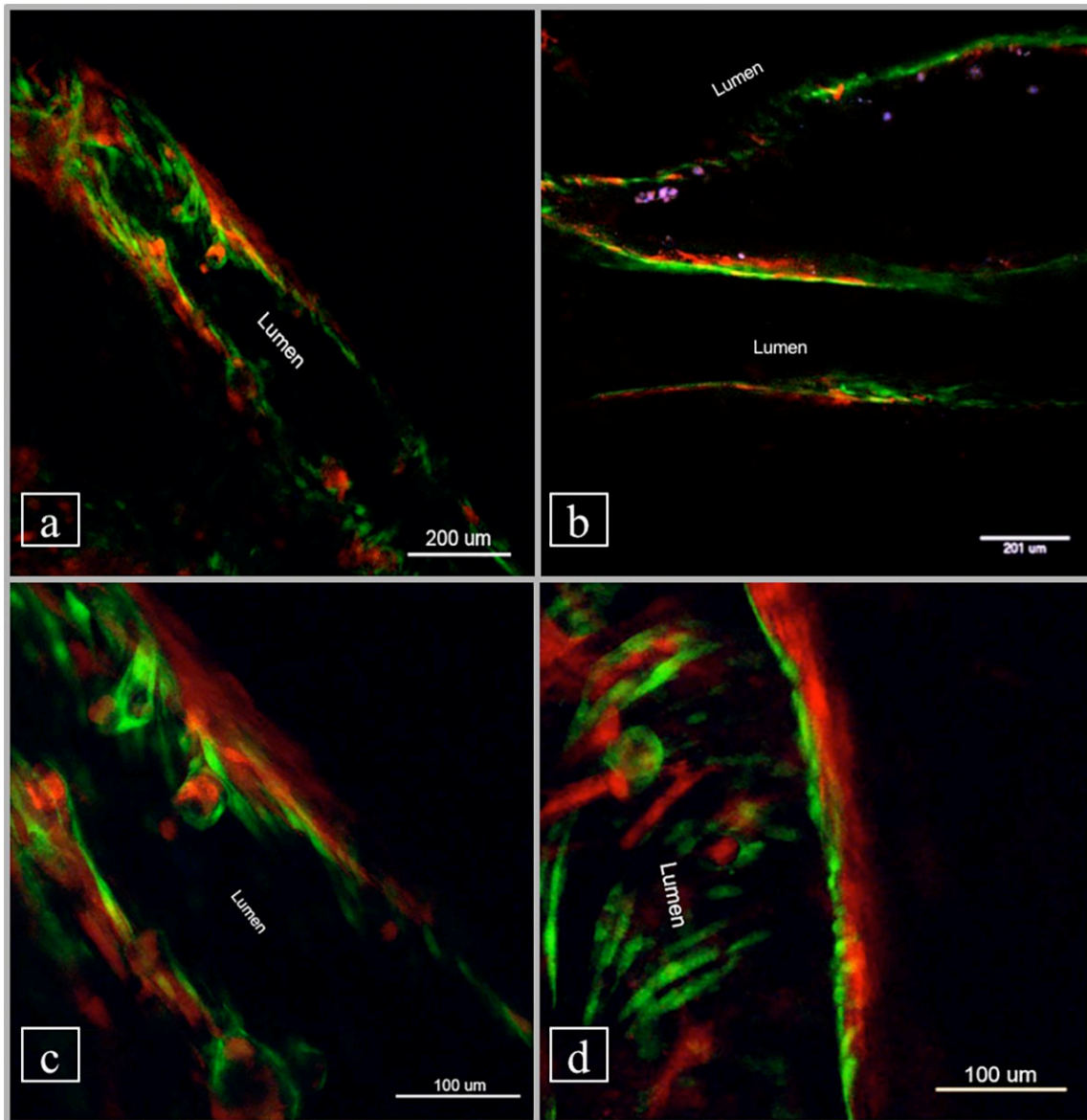
Figure 9: Pre-Vascularized Microvessels at 14 Days of Culture.
a) 10x/0.6NA water immersion objective MPM imaging of microchannel lined with HUVEC-GFP and HASMC-RFP. **b)** 10x/0.6NA water immersion objective MPM imaging of two adjacent microchannels lined with HUVEC-GFP and HASMC-RFP with supporting HPLP- CFP. **c)** 10x/0.6NA water immersion objective with an optical zoom of 3 MPM imaging of same microchannel in image A. **d)** 10x/0.6NA water immersion objective with an optical zoom of 3 MPM imaging of same microchannel in image C demonstrating the formation of a HUVEC-GFP neointima and HASMC-RFP neomedia.
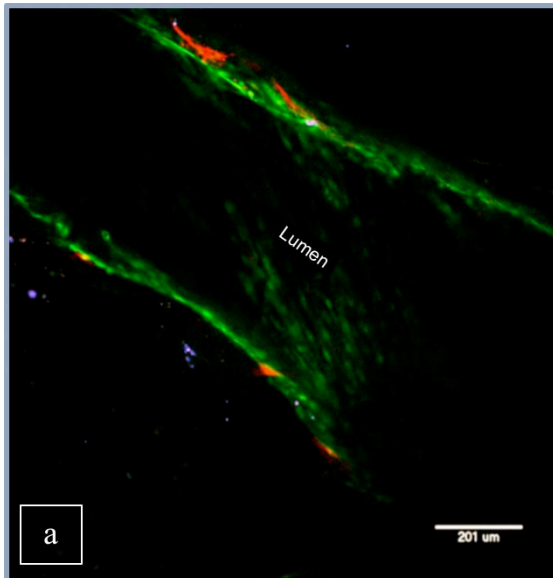
Figure 10a. Pre-Vascularized Microvessel at 14 Days of Culture (Full View): 10x/0.6NA water immersion objective MPM image of a two-walled microchannel lined with HUVEC-GFP and with supporting HASMC-RFP and HPLP-CFP.
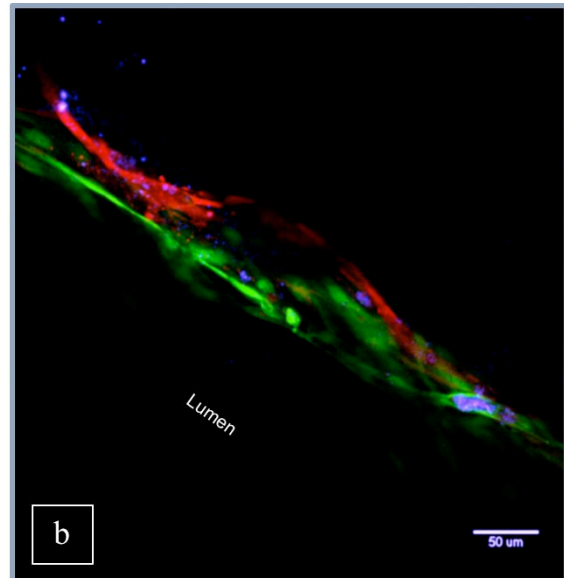
Figure 10b. Pre-vascularized Microvessel (single wall): 10x/0.6NA water immersion objective with an optical zoom of 3 MPM image of figure 10a. Notice the close interaction between the HUVEC-GFP and supporting HASMC-RFP and HPLP-CFP.
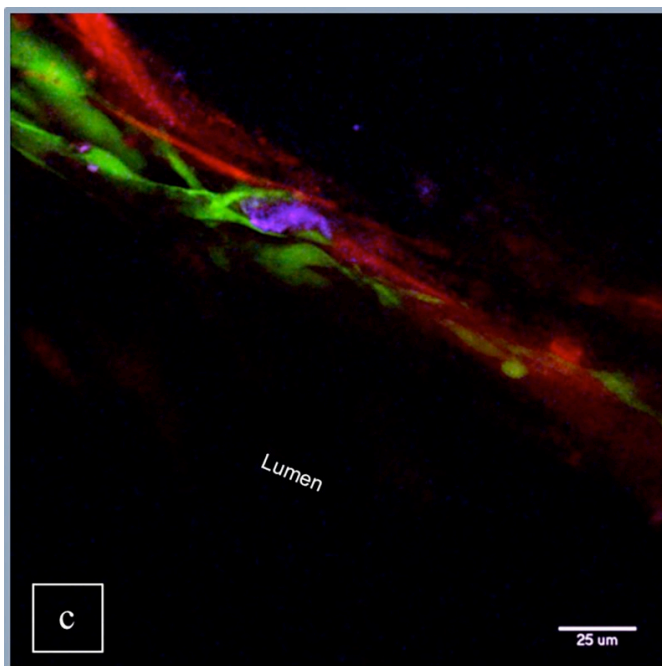
Figure 10c. Pre-vascularized Microvessel (single wall): 10x/0.6NA water immersion objective with an optical zoom of 6 MPM image of figure 10b.

26
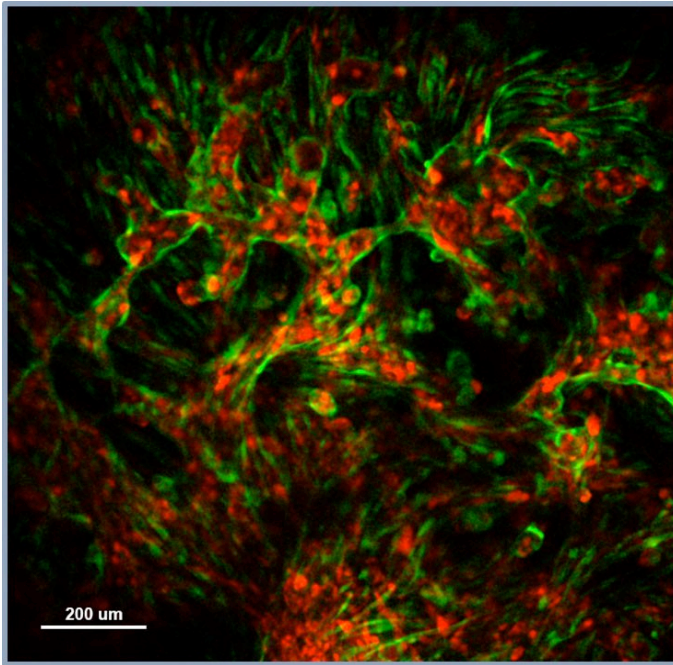
Figure 11. Sprouting Morphogenesis: 10X 0.6/NA water immersion MPM imaging of sprouting morphogenesis within the pre-vascularized skin flap following 14 days of culture. Notice HUVEC-GFP cells and supporting HASMC-RFP cells.
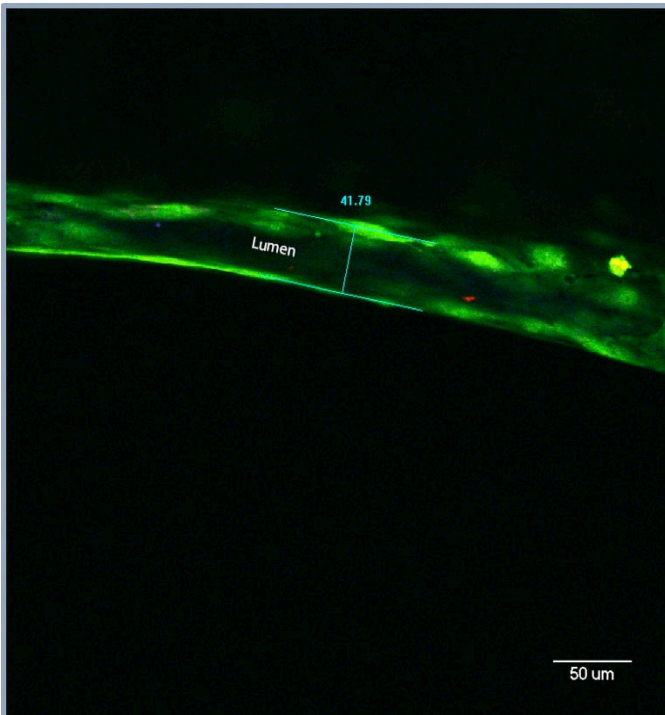
Figure 12. Neovessel Lumen at 28 Days of Culture: 10x/0.6NA water immersion objective with an optical zoom of 3 of MPM imaging of HUVEC-GFP neovessel

(Diameter = 41.79 μm).

27
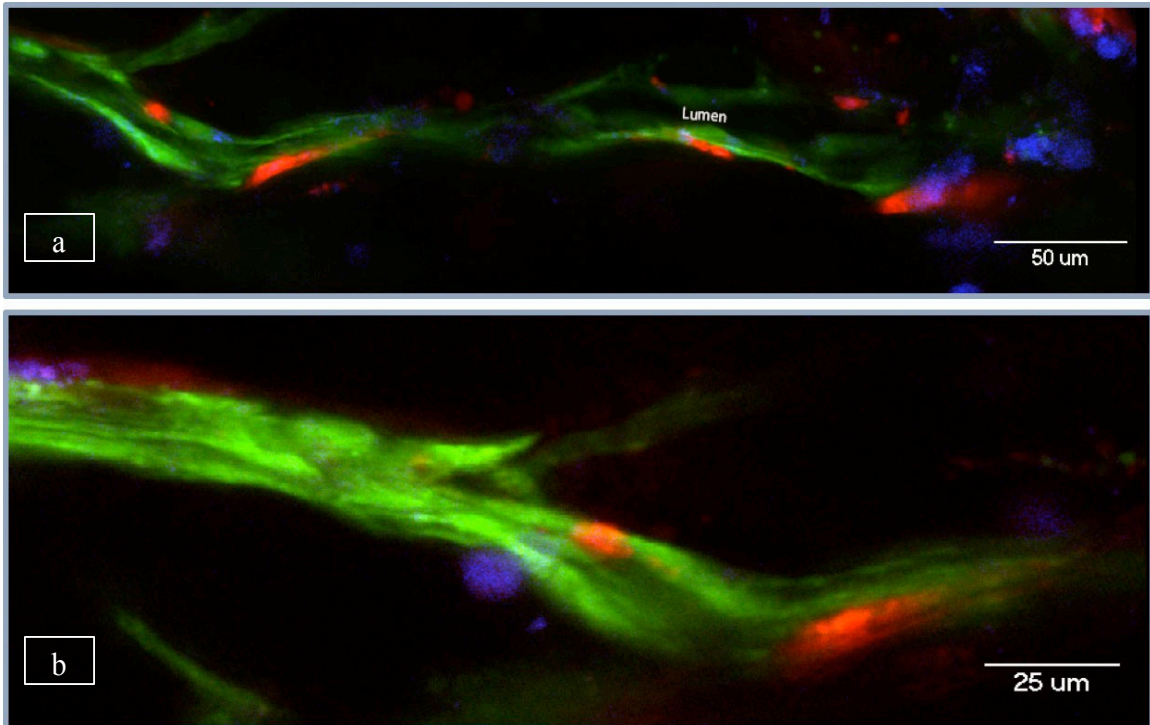
Figure 13. Neovessel Formation at 28 Days of Culture: a) 10x/0.6NA water immersion objective with an optical zoom of 3 of MPM imaging of a neovessel lined with HUVEC-GFP and supporting HASMC-RFP and HPLP-CFP following 28 days of culture. **b)** 10x/0.6NA water immersion objective with an optical zoom of 6 for the same neovessel.

Following purification by sorting of HUVECs from the polyculture environment found within the original collagen hydrogel sample, qPCR was performed to determine the relative RNA expression of markers for endothelial sprouting, angiogenesis and vasculogenesis at 14 and 28 days. Jagged1, Dll4, VE-Cadherin, CD31 and alpha-SMA were compared and normalized to the 18S rRNA reference gene. Expression of CD31 and VE-Cadherin accompanied by a lack of a-SMA expression confirmed the presence of HUVECs in the purified samples at 14 and 28 days. Additionally, qPCR results suggest that two Notch ligands, Jagged1 and Dll4, may have opposing roles during tube formation: at the 14 day time point, Jagged1expression is up relative to Dll4 expression;

at the 28 day time point, Jagged 1 expression is down relative to Dll4 (Figure 14a-b), a phenomenon which has been reported elsewhere (Benedito et al., 2009). Our results shown here suggest this interplay between the various Notch ligands may help regulate the progression of vasculogenesis in a 3-D like environment.

Figure 14. RT-qPCR Analysis for Endothelial Gene Expression: a) Relative gene expression (AU) of CD31, VE-Cadherin and a-SMA of ECs purified from cellularized collagen skin hydrogels at day 14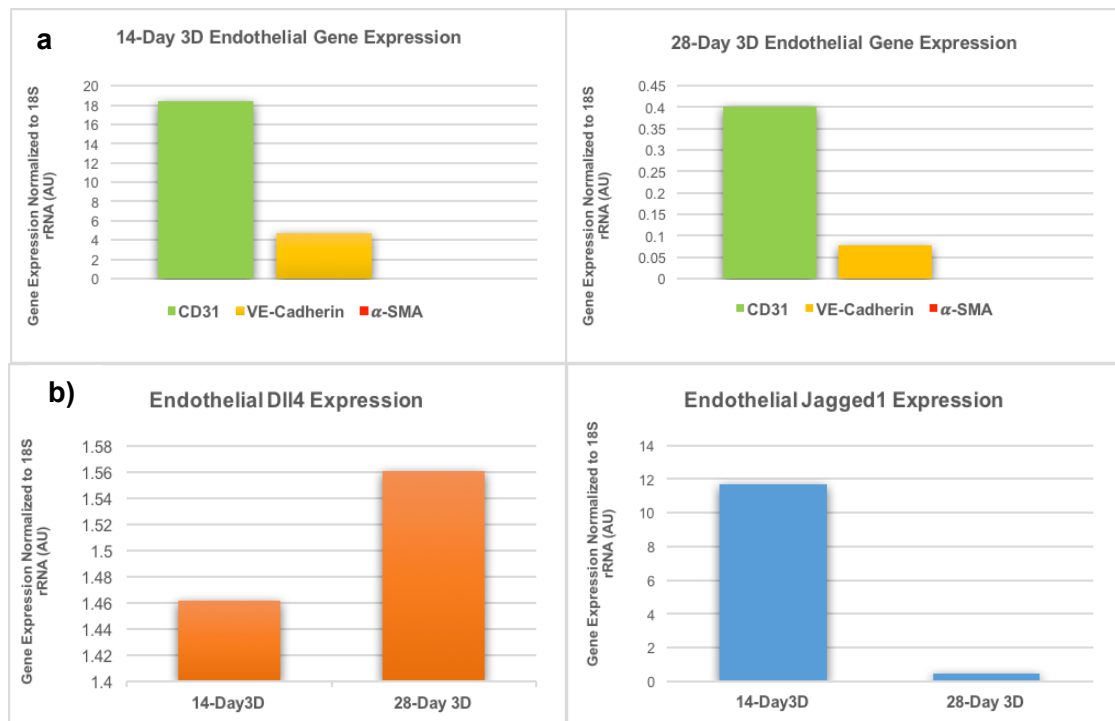 and 28. Expression levels normalized to 18S rRNA. **b)** Relative gene expression (AU) of Dll4 and Jagged 1 of ECs purified from cellularized collagen skin hydrogels at day 14 and 28. Expression levels normalized to 18S rRNA.

DISCUSSION

The present research was intended to fabricate a tissue engineered pre-vascularized skin flap with an inherent network of interconnecting branching vessels capable of providing whole tissue perfusion for immediate clinical applicability. To do so, we utilized our novel technique, which relies on sacrificial polymers to fabricate the intricate network of branching vessels within a biocompatible cellularized collagen matrix. These pre- fabricated channels were then seeded with endothelial and smooth muscle cells re-creating the non-thrombogenic lining of the microvasculature. The surrounding collagen matrix, encapsulated with pericytes and fibroblasts and topically seeded with keratinocytes, simulated the unique cellular environment of *in vivo* skin providing key spatial information for cell localization, proliferation, angiogenesis and vasculogenesis.

As a plastic surgeon's approach to autologous tissue transfer is limited by the availability of autologous tissue and patient donor site morbidity, there remains an urgent need for the development of a tissue engineered full thickness skin flap containing an inherent vascular supply capable of providing immediate whole tissue perfusion (Saint-Cyr et al. 2012). Our proposed tissue engineered pre-vascularized full thickness skin equivalent serves as a novel approach aimed at addressing the limitations currently experienced in the field of plastic and reconstructive surgery.

As cells can only survive within an area approximately 200-300μm away from a nutrient or oxygen source, the fabrication of thicker tissue engineered skin substitutes with an intricate vascular bed of branching vessels that recapitulates the complex   hierarchical

organization of human skin continues to pose a major obstacle (Baptista et al., 2011; Folkman & Hochberg, 1973; Green, 1941). There has been significant research focused on recapitulating the unique microenvironmental conditions within biocompatible matrices to provide cells the necessary stimulus to spontaneously assemble into intricate networks of branching microvessels (Koh et al., 2008; Sacharidou, Stratman, & Davis, 2012; Zheng et al., 2012). However, while such research is successful at developing *de novo* microvessels within biocompatible scaffolds, these approaches fails to employ methods that consider the architecture necessary for microsurgical anastomosis to recipient vasculature, minimizing their clinical translatability.

Furthermore, research focused on pre-fabricating microvessels within biocompatible scaffolds utilizes mandrel molds or soft lithography stamps. This approach, while successful at fabricating small microvessels lined with vascular and mural cells are inefficient at producing larger vessels, which are essential for perfusing large tissue volumes with minimal vascular resistance (Huang et al., 2012; Liu et al., 2012; Rayatpisheh et al., 2014; Wang et al., 2013; Yu & Zhou, 2013). Herein, we combine multiple approaches to create a complex collagen bulk microenvironment, which stimulates spontaneous vascular self-assembly through endothelial/mural polycultures and contains inherent pre- fabricated vessels of scalable size with the appropriate architecture necessary for microsurgical anastomosis to provide large tissue perfusion.

We first reported our approach utilizing sucrose and silicone as the sacrificial and bulk materials, respectively, to generate perfusable microchannels (Bellan et al., 2009). This technique while efficient at fabricating an intricate network of

31

branching microvessels, was not directly translatable because of a lack of scaffold biocompatibility. Additionally, we explored the use of Kerria Lacca Resin (Shellac) as our sacrificial material due to its ability to enable fabrication of a denser tangle of smaller microchannels representative of native *in vivo* capillary networks (Jacoby, in press). However, the method used to sacrifice the shellac is toxic to cells within the collagen bulk therefore restricting its use. We have since focused our efforts on scaffold material chemistry to employ the use of Pluronic® F127, our sacrificial microfiber. FDA approved and commonly found in cosmetics, Pluronic® F127 is a tri-block copolymer containing a central hydrophobic core of polypropylene glycol flanked by hydrophilic polyethylene glycol, and here it is used to form the microchannels within our matrix (Kabanov et al., 2002). To encourage cellular survival and subsequent scaffold integration within the host, type-I collagen was replaced as the ideal bulk material as it its an integral component of the natural ECM, has low antigenicity, is biodegradable, biocompatible, and facilitates cellular adhesion and growth (Cross et al., 2010; Hooper et al., 2014).

Mediated by the notch pathway, sprouting angiogenesis is a tightly regulated process that requires a coordinated balance between notch ligands Dll4 and Jagged 1 (Benedito et al., 2009). Endothelial tip cells lead the outgrowth of blood vessel sprouts by sensing and responding to environmental cues such as vascular endothelial growth factor- A (VEGF-A), while stalk cells are located more distally from the gradient. The endothelial expression patterns of tip cell expressing Dll4 and stalk cell expressing Jagged 1 experience a mosaic pattern of expression (Hellström et al., 2007; High et al., 2008).

Adams et al., previously demonstrated that the equilibrium between the two ligands can be controlled by Dll4 expression in endothelial tip cells, which activates Notch signaling and thereby suppresses sprouting in adjacent endothelial cells. In turn, stalk cells expressing Jagged 1 antagonize tip cells expressing Dll4 promoting sprouting angiogenesis. It is the suppression of the tip cell phenotype, which may in turn promote tubulogenesis (Roca & Adams, 2007). This evidence parallels Harrington et al., findings, which suggest that HUVEC expressing Dll4 inhibits sprouting formation bringing an end to the initial proliferative phase of angiogenesis triggering a maturation phase to refine and stabilize new vessel vascular function. Our results herein, indicate a mosaic like environment of Dll4 and Jagged 1 expression at 14 and 28 days furthering the possibility of earlier periods of sprouting angiogenesis followed by a period of vessel maturation. While the relationship between endothelial expression of Jagged 1 and Dll4 is not fully elucidated as of yet in a three-dimensional model, our proposed tissue- engineered skin flap holds promise for future studies delineating this relationship under physiological conditions recapitulating an *in vivo* environment.

Close communication with the underlying mural cells are required to ensure stability and viability of endothelial capillary networks, as we and others have shown that co-seeding endothelial with smooth muscle cells supports sprouting, vessel stability and maturation (Hooper et al., 2014; Lilly, 2014; Liu et al., 2012). Sefton *et al.* indicate that the presence of smooth muscle cells induce endothelial expression of Ve-Cadherin, which is crucial to the to development of cell-cell adherent junctions, the formation of a stable confluent functional lining and a non-thrombogenic endothelial surface (Chiu et

al., 2009; Matter & Balda, 2003). Following 14 days and 28 days of culture, real-time qPCR confirmed relative expression of Ve-Cadherin from isolated endothelial cells indicating the development and maintenance of a functional non-thrombogenic endothelium within our pre-fabricated microvessels.

The presence of pericytes are a crucial component of the endothelial vasculature as their recruitment during vasculogenesis and angiogenesis stabilizes and supports the function of blood flow in early developing capillaries (Franco et al., 2011; Stratman & Davis, 2012). Utilizing cyan fluorescent protein, we tagged the pericytes used in our study to clearly and unmistakably identify their location within the vasculature. MPM imaging revealed that in smaller microvessels, pericytes were located sub adjacent to the tunica media smooth muscle layer while remaining in close contact with the tunica intima endothelial layer. These findings are indicative of endothelial driven pericyte recruitment, and of the supportive role pericytes play in the development of a vascularized endothelium (Gerhardt et al., 2003; Song et al., 2005; Stratman & Davis, 2012). Building upon our previous work where we combine the fields of biology, polymer chemistry, and engineering, we sought to fabricate a three-dimensional tissue engineered full thickness skin equivalent containing an inherent network of patent and vascularized interconnecting vessels capable of microsurgical anastomosis to recipient vasculature. We employ methods that take advantage of the unique elements of human skin to ensure proper signaling within our bio-scaffold environment to promote a healthy, proliferative and stable vasculature. While current approaches to tissue-engineered skin equivalents face the challenge of producing macro-scale vascular networks and the

34

primary branch order networks, both of which are essential for perfusing whole large tissue volumes with minimal vascular resistance, our approach represents a significant advancement in the fabrication of surgically-relevant replacement tissues. Because of its internal microvasculature and readily available anastomosis architecture, our constructs are able to provide whole tissue perfusion and therefore present as an alternate approach to currently available tissue engineered skin equivalents that rely upon scaffold engraftment via the host wound bed.

Future work will require that we perform anastomosis of our proposed tissue engineered skin flaps on animal models to provide conclusive evidence of its clinical feasibility. Alternatively, as our tissue engineered constructs closely mimic the *in vivo* architecture and environment of human skin they have the ability to serve as a unique platform to study mechanistic actions of certain cancers and tumors. Our results demonstrate a foreseeable translation to the clinic with the hope of offering the first ever *de novo* designable vascularized tissue that eliminates the need for autologous harvest.

REFERENCES

Adams, D. C., & Ramsey, M. L. (2005). Grafts in dermatologic surgery: review and update on full- and split-thickness skin grafts, free cartilage grafts, and composite grafts. *Dermatologic Surgery*, *31*(8 Pt 2), 1055–1067.

Andreassi, A., Bilenchi, R., Biagioli, M., & D'Aniello, C. (2005). Classification and pathophysiology of skin grafts. *Clinics in Dermatology*, *23*(4), 332–337.

Baek, K., Jeong, J. H., Shkumatov, A., Bashir, R., & Kong, H. (2013). In situ self-folding assembly of a multi-walled hydrogel tube for uniaxial sustained molecular release. *Advanced Materials*, *25*(39), 5568–5573.

Baptista, P. M., Siddiqui, M. M., Lozier, G., Rodriguez, S. R., Atala, A., & Soker, S. (2011). The use of whole organ decellularization for the generation of a vascularized liver organoid. *Hepatology*, *53*(2), 604–617.

Bellan, L. M., Singh, S. P., Henderson, P. W., Porri, T. J., Craighead, H. G., & Spector, J. A. (2009). Fabrication of an artificial 3-dimensional vascular network using sacrificial sugar structures. *Soft Matter*, *5*(7), 1354.

Benedito, R., Roca, C., Sörensen, I., Adams, S., Gossler, A., Fruttiger, M., & Adams, R.H. (2009). The notch ligands Dll4 and Jagged1 have opposing effects on angiogenesis. *Cell*, *137*(6), 1124–1135.

Berthiaume, F., Maguire, T. J., & Yarmush, M. L. (2011). Tissue engineering and regenerative medicine: history, progress, and challenges. *Annual Review of Chemical and Biomolecular Engineering*, *2*, 403–30.

Blinder, Y., Mooney, D., & Levenberg, S. (2014). Engineering approaches for inducing blood vessel formation. *Current Opinion in Chemical Engineering*, *3*, 56–61.

Boyce, D. E., & Shokrollahi, K. (2006). Reconstructive surgery. *BMJ: British Medical Journal, 332*(7543), 710–2.

Callcut, R. A., Schurr, M. J., Sloan, M., & Faucher, L. D. (2006). Clinical experience with Alloderm: a one-staged composite dermal/epidermal replacement utilizing processed cadaver dermis and thin autografts. *Burns: Journal of the International Society for Burn Injuries*, *32*(5), 583–588.

Chapter 2 grafts and flaps. (n.d.). Retrieved from http://www.plasticsurgery.org/Documents/medical-professionals/publications/Essentials-Chapter-2-Grafts-and-Flaps.pdf

Chen, T.-H., Zhu, X., Pan, L., Zeng, X., Garfinkel, A., Tintut, Y., … Ho, C.-M. (2012). Directing tissue morphogenesis via self-assembly of vascular mesenchymal cells. *Biomaterials*, *33*(35), 9019–26.

Chiu, Y.-J., Kusano, K., Thomas, T. N., & Fujiwara, K. (2009). Endothelial cell-cell adhesion and mechanosignal transduction. *Endothelium: Journal of Endothelial Cell Research*, *11*(1), 59–73.

Cross, V. L., Zheng, Y., Won Choi, N., Verbridge, S. S., Sutermaster, B. A., Bonassar, L. J., … Stroock, A. D. (2010). Dense type I collagen matrices that support cellular remodeling and microfabrication for studies of tumor angiogenesis and vasculogenesis in vitro. *Biomaterials*, *31*(33), 8596–607.

Devices, P. S. (2000). Tissue engineering. *Nature Biotechnology*, *18*(Suppl. 2000), IT56–IT58. doi:10.1038/80103

Ehsan, S. M., Welch-Reardon, K. M., Waterman, M. L., Hughes, C. C. W., & George, S. C. (2014). A three-dimensional in vitro model of tumor cell intravasation. *Integrative Biology*, *6*(6), 603–610.

Fimiani, M., Pianigiani, E., Di Simplicio, F. C., Sbano, P., Cuccia, A., Pompella, G., …Petraglia, F. (2005). Other uses of homologous skin grafts and skin bank bioproducts. *Clinics in Dermatology*, *23*(4), 396–402.

Folkman, J., & Hochberg, M. (1973). Self-regulation of growth in three dimensions. *Journal of Experimental Medicine*, *138*(4), 745–53.

Franco, M., Roswall, P., Cortez, E., Hanahan, D., & Pietras, K. (2011). Pericytes promote endothelial cell survival through induction of autocrine VEGF-A signaling and Bcl- w expression. *Blood*, *118*(10), 2906–17.

Free Tissue Transfer Flaps: Definition, Indications, Preoperative Considerations. (n.d.). Retrieved January 31, 2016, from

http://emedicine.medscape.com/article/1284841- overview#a1

Gauvin, R., Ahsan, T., Larouche, D., Lévesque, P., Dubé, J., Auger, F. A., … Germain, L. (2010). A novel single-step self-assembly approach for the fabrication of tissue-engineered vascular constructs. *Tissue Engineering. Part A*, *16*(5), 1737–1747.

Gerhardt, H., Golding, M., Fruttiger, M., Ruhrberg, C., Lundkvist, A., Abramsson, A., … Betsholtz, C. (2003). VEGF guides angiogenic sprouting utilizing endothelial

tip cell filopodia. *Journal of Cell Biology*, *161*, 1163–1177.

Golden, A. P., & Tien, J. (2007). Fabrication of microfluidic hydrogels using molded gelatin as a sacrificial element. *Lab on a Chip*, *7*(6), 720–725.

Greene, H. S. (1941). Heterologous transplantation of mammalian tumors II: the transfer of human tumors to alien species. *Journal of Experimental Medicine*, *73*(4), 475–486.

Hasan, A., Paul, A., Vrana, N. E., Zhao, X., Memic, A., Hwang, Y.-S., … Khademhosseini, A. (2014). Microfluidic techniques for development of 3D vascularized tissue. *Biomaterials*, *35*(26), 7308–25.

Hellström, M., Phng, L.-K., Hofmann, J. J., Wallgard, E., Coultas, L., Lindblom, P., … Betsholtz, C. (2007). Dll4 signalling through Notch1 regulates formation of tip cells during angiogenesis. *Nature*, *445*(7129), 776–780.

High, F. A., Lu, M. M., Pear, W. S., Loomes, K. M., Kaestner, K. H., & Epstein, J. A. (2008). Endothelial expression of the Notch ligand Jagged1 is required for vascular smooth muscle development. *Proceedings of the National Academy of Sciences of the United States of America*, *105*(6), 1955–1959.

Hooper, R. C., Hernandez, K. a, Boyko, T., Harper, A., Joyce, J., Golas, A. R., & Spector, J. a. (2014). Fabrication and in vivo microanastomosis of vascularized tissue-engineered constructs. *Tissue Engineering. Part A*, *20*(19-20), 2711–2719.

Hoying, J. B., Utzinger, U., & Weiss, J. A. (2014). Formation of microvascular networks: role of stromal interactions directing angiogenic growth. *Microcirculation*, *21*(4), 278–289.

Huang, Z., Li, X., Martins-Green, M., & Liu, Y. (2012). Microfabrication of cylindrical microfluidic channel networks for microvascular research. *Biomedical Microdevices*, *14*(5), 873–883.

Jiang, L.-Y., & Luo, Y. (2013). Guided assembly of endothelial cells on hydrogel matrices patterned with microgrooves: a basic model for microvessel engineering. *Soft Matter*, *9*(4), 1113–1121.

Kabanov, A. V, Lemieux, P., Vinogradov, S., & Alakhov, V. (2002). Pluronic block copolymers: novel functional molecules for gene therapy. *Advanced Drug Delivery Reviews*, *54*(2), 223–233.

Kannan, R. Y., Salacinski, H. J., Sales, K., Butler, P., & Seifalian, A. M. (2005). The roles of tissue engineering and vascularisation in the development of micro-vascular networks: a review. *Biomaterials*, *26*(14), 1857–1875.

Kim, J., Yang, K., Park, H.-J., Cho, S.-W., Han, S., Shin, Y., … Lee, J. H. (2014). Implantable microfluidic device for the formation of three-dimensional vasculature by human endothelial progenitor cells. *Biotechnology and Bioprocess Engineering*, *19*(3), 379–385.

Koh, W., Stratman, A. N., Sacharidou, A., & Davis, G. E. (2008). In vitro three dimensional collagen matrix models of endothelial lumen formation during vasculogenesis and angiogenesis. *Methods in Enzymology*, *443*, 83–101.

Kojima, K., Bonassar, L. J., Roy, A. K., Vacanti, C. A., & Cortiella, J. (2002). Autologous tissue-engineered trachea with sheep nasal chondrocytes. *Journal of Thoracic and Cardiovascular Surgery*, *123*(6), 1177–1184.

Kolesky, D. B., Truby, R. L., Gladman, A. S., Busbee, T. A., Homan, K. A., & Lewis, J.A. (2014). 3D bioprinting of vascularized, heterogeneous cell-laden tissue constructs. *Advanced Materials*, *26*(19), 3124–3130.

Lee, Y. Bin, Jun, I., Bak, S., Shin, Y. M., Lim, Y.-M., Park, H., & Shin, H. (2014). Reconstruction of vascular structure with multicellular components using cell transfer printing methods. *Advanced Healthcare Materials*, *3*(9), 1465–1474.

Lilly, B. (2014). We have contact: endothelial cell-smooth muscle cell interactions. *Physiology*, *29*(4), 234–241.

Lin, R.-Z., Chen, Y.-C., Moreno-Luna, R., Khademhosseini, A., & Melero-Martin, J. M. (2013). Transdermal regulation of vascular network bioengineering using a photopolymerizable methacrylated gelatin hydrogel. *Biomaterials*, *34*(28), 6785–96.

Liu, Y., Rayatpisheh, S., Chew, S. Y., & Chan-Park, M. B. (2012). Impact of endothelial cells on 3D cultured smooth muscle cells in a biomimetic hydrogel. *ACS Applied Materials & Interfaces*, *4*(3), 1378–1387.

Lokmic, Z., Stillaert, F., Morrison, W. A., Thompson, E. W., & Mitchell, G. M. (2007). An arteriovenous loop in a protected space generates a permanent, highly vascular, tissue-engineered construct. *FASEB Journal*, *21*(2), 511–522.

Matter, K., & Balda, M. S. (2003). Functional analysis of tight junctions. *Methods*, *30*(3), 228–234.

Miller, J. S., Stevens, K. R., Yang, M. T., Baker, B. M., Nguyen, D.-H. T., Cohen, D. M., Chen, C. S. (2012). Rapid casting of patterned vascular networks for

perfusable engineered three-dimensional tissues. *Nature Materials*, *11*(9), 768–774.

Novosel, E. C., Kleinhans, C., & Kluger, P. J. (2011). Vascularization is the key challenge in tissue engineering. *Advanced Drug Delivery Reviews*, *63*(4-5), 300–311.

Patterson, D. R., Everett, J. J., Bombardier, C. H., Questad, K. A., Lee, V. K., & Marvin, J. A. (1993). Psychological effects of severe burn injuries. *Psychological Bulletin*, *113*(2), 362–378.

Pećanac, M. Đ. (2015). Development of plastic surgery. *Medicinski Pregled*, *68*(5-6), 199–204.

Rayatpisheh, S., Heath, D. E., Shakouri, A., Rujitanaroj, P.-O., Chew, S. Y., & Chan-Park, M. B. (2014). Combining cell sheet technology and electrospun scaffolding for engineered tubular, aligned, and contractile blood vessels. *Biomaterials*, *35*(9), 2713–2719.

Reiffel, A. J., Sohn, A. M., Henderson, P. W., Fullerton, N., & Spector, J. A. (2012). Use of Integra and interval brachytherapy in a 2-stage auricular reconstruction after excision of a recurrent keloid. *Journal of Craniofacial Surgery*, *23*(5), e379–380.

Roca, C., & Adams, R. H. (2007). Regulation of vascular morphogenesis by Notch signaling. *Genes & Development, 21*(20), 2511–2524.

Sacharidou, A., Stratman, A. N., & Davis, G. E. (2012). Molecular mechanisms controlling vascular lumen formation in three-dimensional extracellular

matrices. *Cells, Tissues, Organs*, *195*(1–2), 122–143.

Saint-Cyr, M. Wong, C., Buchel, E.W., Colohan, S., Pederson, W.C. (2012). Free tissue transfers and replantation. *Plastic and Reconstructive Surgery*, *130*(6), 858e–878e. doi: 10.1097/PRS.0b013e31826da2b7

Sen, C. K., Gordillo, G. M., Roy, S., Kirsner, R., Lambert, L., Hunt, T. K., … Longaker, M. T. (2009). Human skin wounds: A major and snowballing threat to public health and the economy. *Wound Repair and Regeneration*, *17*(6), 763–771.

Song, J. W., Gu, W., Futai, N., Warner, K. a, Nor, J. E., & Takayama, S. (2005). Computer-controlled microcirculatory support system for endothelial cell culture and shearing. *Analytical Chemistry*, *77*(13), 3993–3999.

Stratman, A. N., & Davis, G. E. (2012). Endothelial cell-pericyte interactions stimulate basement membrane matrix assembly: influence on vascular tube remodeling, maturation, and stabilization. *Microscopy and Microanalysis*, *18*(1), 68–80.

The economic cost of wounds | Smith & Nephew. (n.d.). Retrieved May 10, 2016 from http://www.smith-nephew.com/about-us/what-we-do/advanced-wound-management/economic-cost-of-wounds/

Tremblay, P.-L., Hudon, V., Berthod, F., Germain, L., & Auger, F. A. (2005). Inosculation of tissue-engineered capillaries with the host's vasculature in a reconstructed skin transplanted on mice. *American Journal of Transplantation*, *5*(5), 1002–10.

Wang, J.-C., Tu, Q., Wang, Y., Liu, W., Liu, R., Shen, S., … Wang, J. (2013). Pneumatic mold-aided construction of a three-dimensional hydrogel

microvascular network in an integrated microfluidics and assay of cancer cell adhesion onto the endothelium. *Microfluidics and Nanofluidics*, *15*(4), 519–532.

Wu, X., Rabkin-Aikawa, E., Guleserian, K. J., Perry, T. E., Masuda, Y., Sutherland, F. W. H., … Bischoff, J. (2004). Tissue-engineered microvessels on three-dimensional biodegradable scaffolds using human endothelial progenitor cells. *American Journal of Physiology. Heart and Circulatory Physiology*, *287*(2), H480–487.

Yu, H., & Zhou, G. (2013). Deformable mold based on-demand microchannel fabrication technology. *Sensors and Actuators B: Chemical*, *183*, 40–45.

Zheng, Y., Chen, J., Craven, M., Choi, N. W., Totorica, S., Diaz-Santana, A., … Stroock, A. D. (2012). In vitro microvessels for the study of angiogenesis and thrombosis. *Proceedings of the National Academy of Sciences of the United States of America*, *109*(24), 9342–9347.

Zhong, S. P., Zhang, Y. Z., & Lim, C. T. (2010). Tissue scaffolds for skin wound healing and dermal reconstruction. *Wiley Interdisciplinary Reviews. Nanomedicine and Nanobiotechnology*, *2*(5), 510–525.

CURRICULUM VITAE

ROSS H. WEINREB

300 East 56th Street, New York, NY 10022 •
rossweinreb@gmail.com • 516.835.1100.
YOB: 1991

EDUCATION

Boston University School of Medicine   **Boston, MA**
Candidate for Master of Science in Medical Science   *08/14 – 05/16*

The Pennsylvania State University – Eberly College of Science   **State College, PA**
B.S. Major in Biological Sciences Health Professions & Minor in Psychology   *08/10 – 05/14*
- Cumulative GPA: 3.67
- Honors: Sigma Alpha Mu Young Scholar's Award, Dean's List, Alpha Sigma Pi Honors Society
- Penn State Club Lacrosse

PROFESSIONAL EXPERIENCE

MEDLIFE Mobile Medical Clinic   **Riobamba, Ecuador**
Medical Mission Volunteer   *08/12*
- Assisted local doctors with treatment and follow up care for individuals and families who lack access to medical services
- Facilitated medical and dental education programs to educate locals on relevant health topics including diabetes

Beth Israel Hospital – Department of Sports Medicine Services   **New York, NY**
Medical Intern with Jerry Lubliner M.D., Chief of Sports Medicine Services   *06/11 – 08/11*
- Shadowed Dr. Lubliner and team in the operating room for 3-6 operations per week
- Aided in daily patient consults and gathered statistics on patient charts to assist the medical staff

North Shore LIJ Hospital – Department of Cardiovascular Surgery   **Manhasset, NY**
Co-op with Alan Hartman M.D., Chairman of Cardiothoracic Surgery   *01/09 – 06/10*
- Observed bedside procedures, patient rounds and critical care treatments in the cardiothoracic surgical intensive care unit
- Witnessed daily hospital operational management within the cardiothoracic surgical intensive care unit

RESEARCH EXPERIENCE

Weill Cornell Medicine – New York Presbyterian Hospital   **New York, NY**
Graduate Fellow in The Laboratory for Bioregenerative Medicine & Surgery, Jason A. Spector, M.D.   *Present*
- Use collagen hydrogels to fabricate pre-vascularized full thickness tissue-engineered skin with an inherent vascular network for immediate clinical translation, with the goal of creating the first ever tissue engineered pre-vascularized perfusable skin flap
- Utilize 3D printing technology to fabricate tissue-engineered human ears to target the Microtia patient population
- Development of a portable non-thermal plasma device that provides rapid and efficient bactericidal sterilization of patient infected wound beds
- Fabricate pre-vascularized tissue engineered skin to study tumorigenesis/metastasis using breast cancer cells (MDAMB231)

The Feinstein Institute for Medical Research – Northwell Health System   **Manhasset, NY**
Research Scholar in The Laboratory of Papillomavirus Research, Bettie Steinberg Ph.D.   *06/12 – 08/12*
- Optimized 3-D raft cultures of ROCK inhibited laryngeal keratinocytes to observe inhibitory effects on Rac-1 and associated COX-2 expression in Recurrent Respiratory Papillomavirus
- Modified early gene expression in HPV11 to identify the HPV causing gene

The Pennsylvania State University   **State College, PA**
Research Assistant in The Pathways to Alzheimer's Research, Robert W. Schrauf, Ph.D.   *09/10 – 01/11*
- Investigated an association between patient families to detect the early onset symptoms of Alzheimer's disease
- Organized and compiled data to create data trends and specific coding sequences

LEADERSHIP EXPERIENCE

MEDLIFE PSU Chapter   **State College, PA**
Founder & Co-President   *01/12 – 05/14*
- Proposed, created, and implemented a MEDLIFE chapter on the Penn State campus
- Provided undergraduates the opportunity to be a part of MEDLIFE mobile clinics abroad

Sigma Alpha Mu Fraternity   **State College, PA**
Executive Counsel: Recorder & VP Philanthropy   *11/11 – 01/13*
- Managed all legal and community relations regarding the Mu Lambda chapter
- Coordinated philanthropic events to raise over $120,000 annually for Penn State THON